



RESEARCH ARTICLE

BONEMODELING USING THE MORTON SPACE-FILLING CURVE

¹José P. Suárez, ²Daniel R. Hernández, ³A. Plaza and ¹Abad, P.

¹PhD, Applied Mathematics, Cartography and Graphic Engineering Department 35017 Las Palmas de Gran Canarias. Spain

²PhD Mechanical Engineering, Mechanical and Industrial Engineering Department Antonio Nariño University, Neiva, Colombia

³PhD, Applied Mathematics, Mathematics Department 35017 Las Palmas de Gran Canarias. Spain

ARTICLE INFO

Article History:

Received 29th September, 2017
Received in revised form
17th October, 2017
Accepted 22nd November, 2017
Published online 30th December, 2017

Keywords:

Mechanical properties,
Bone modeling,
Space Filling Curve,
CAD Algorithm.

ABSTRACT

We introduce an algorithm for obtaining a geometric bone model suitable for the analysis of bone mechanical properties. In the bone model construction, we use new patterns of the familiar Morton curve, a class of Space Filling Curves. By extending a previous idea for the Hilbert curve, we derive new curve patterns used to construct the space filling curve in the bone model. We show the utility in bone modeling by means of an algorithm that generates the Morton curve and efficiently compute the bone properties such as density, Young's modulus and Poisson's ratio. The algorithm was implemented in AutoLISP language and tested in the AutoCAD system. The algorithm and the new curve patterns offer an efficient tool for analyzing bone properties.

INTRODUCTION

A curve that fills the space or Space filling Curve, from now on SFC, is a continuous mapping from the one-dimensional space onto the bi-dimensional space. That kind of curves has been related with some engineering problems, for example, data structures (R. Pajarola, Antonijuan, and Lario, 2002), ground representations and modelling (Evans, Kirkpatrick, and Townsend, 2001; R. W. Pajarola, Peter, 2001) image compression (R. Pajarola, 2000; Song and Roussopoulos, 2000) and neighbour-finding (Chen and Chang, 2005; Erickson, 1999). Even in the known field of Finite Element Method, SFC's have been an issue of high interest with application for example to refine meshes (Burgarelli, Kischinhevsky, and Biezuner, 2006; Plaza, Suárez, and Padrón, 2005). SFC's are defined explicitly by recursive formulas and very compact and simple algorithms. However the number and shape of the curve patterns created is not obvious or neither simple. Then, some interesting questions arise: how many unique patterns, under rotations and mirror-like reflections are required to describe one of these curves? How is the connection way between filling-space patterns? Answering these questions helps to enhance the application fields of such curves, for example to model geometrically a bone and, in that way, offer new tools for the analysis of the bone mechanical characteristics.

As noted by Sagan (Sagan, 1994), G. Peano (Peano, 1890) discovered the first SFC, but Hilbert was the first one who finds a general geometric procedure that allowed the construction of an entire class of SFC's (Hilbert, 1891). Hilbert held the following heuristic principle: If the interval I can be mapped continuously onto the square Q, then, after subdividing I into four congruent subintervals and Q into other four congruent sub-squares, each subinterval can be mapped continuously onto one of the sub-squares. Next, each subinterval is partitioned again, in turn, into four new congruent subintervals, and each sub-square into congruent sub-squares, so the argument is repeated again and again. If this is carried on infinitum, I and Q are partitioned into 2^{2n} congruent replicas, being $n = 1, 2, 3, \dots$. Hilbert demonstrated that the sub-squares can be arranged so that adjacent subintervals correspond to adjacent sub-squares with a segment in common, and then the inclusion relationship is preserved, i.e., if a square corresponds to an interval, then its sub-squares correspond to the subintervals of that interval. Figure 1 shows the first three steps in the generation of Hilbert's Curve. The curve replicates in four quadrants in the following form, see Figure 1, resolution 3: the lower left quadrant is rotated 90° clockwise; the lower right quadrant is rotated 90° anti-clockwise. The two upper quadrants do not rotate and maintain as quadrants of resolution 2. It is worth to note that all rotation and curve generation are related to the previously obtained in a particular quadrant.

*Corresponding author: José P. Suárez,

¹PhD, Applied Mathematics, Cartography and Graphic Engineering Department 35017 Las Palmas de Gran Canarias. Spain

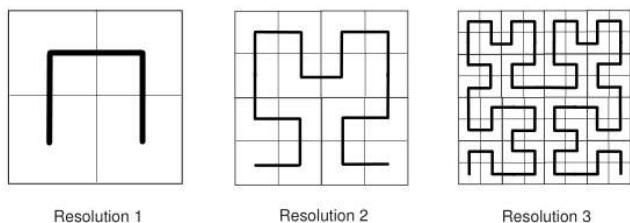


Figure 2. First steps in the generation of Hilbert's Curve

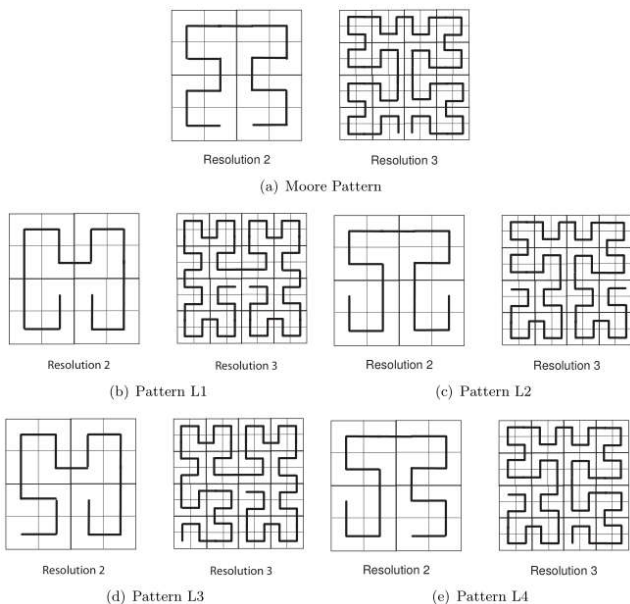


Figure 2. Alternative patterns of the Hilbert curve by Moore and Liu (Liu, 2004)

Moore reported an alternative pattern (Moore, 1900), see Figure 2 (a), and also Liu has recently presented some patterns for the generation of Hilbert-type curves (Liu, 2004), see 2 (b), (e). Liu's patterns, together with Hilbert's original pattern and Moore's pattern, comprise a complete set of the Hilbert's curve (Liu, 2004). Note that all these Hilbert-type patterns, see Figure 2 (a) are reproduced following the relative position determinate by its corresponding pattern to the resolution 2, and the same criteria and way of procedure is applied to upper resolutions. Following the same idea, in this article are proposed new alternatives to the Morton-type Patterns. Morton's Curves have created interest in a range of engineering applications, computers, including PDE solutions by the Finite Elements Method, multigrids, algorithms and programming. Our study establishes utility geometric patterns which also can be applied for bone modeling, as it will be shown later. This article is structured in two parts. In Section 2 we obtain the new patterns of Morton-type, analyzing the possible configurations and the number of equivalent and non-equivalent configurations. The second part of the paper, section 3, describes an algorithm where a bone model is computed from a set of input bone images representing cuts obtained by Computerized Axial Tomography. The bone model so produced is constructed by combining patterns of the Morton's curve. With this algorithm we provide an efficient tool to calculate the bone mechanical properties as Bone Density, Elasticity Modulus and Poisson's Ratio.

Alternative Patterns for the Morton Space Filling Curve

The focus of this paper is the Morton curve and different alternative patterns for it. Like a Hilbert curve, a Morton curve

also has a recursive structure; however, lattice points along a Morton curve are not always adjacent neighbors. This results in a slightly lower degree of locality. Morton curves are popular because they are simple to compute: a point's position along the curve is determined by a bitwise interleaving of its coordinates (Morton, 1966) (bit shuffling on the X and Y coordinates).

The configurations of these patterns can analytically be described in terms of complex algebra. Let C be the complex space. Consider the region $C^+ = \{z \in C | \text{Re}(z) \geq 0, \text{Im}(z) \geq 0\}$. We will construct the concerned patterns in C^+ . Given resolution r, consider a square D with its lower-left corner at the origin and with side 2^r , partitioned into four quadrants which are indexed by 0, 1, 2, and 3, respectively. The sequence 0,1,2,3 in Figure 3 (a) also specifies the pattern of resolution 1 in the Hilbert type curves, while the same sequence in Figure 3 (c) is for the pattern of resolution 1 in the Morton type curves.

The generation of the configuration of pattern from resolution 1 to 2 for the Morton curve given in Figure 4 is determined by the transformations given in Table 1, where the sub-index of the transformation means the quadrant in which the image is, and j is the imaginary number $\sqrt{-1}$:

Table 1. Simple transformations from the original resolution 1 to resolution 2 for the Morton curve

$T_2(z) = \frac{j+z}{2}$	$T_3(z) = \frac{1+j+z}{2}$
$T_0(z) = \frac{z}{2}$	$T_1(z) = \frac{j+z}{2}$

If transformations of Table 1 are recursively applied to pattern Z (reversed) of resolution n, then pattern Z (reversed) of resolution n + 1 is obtained.

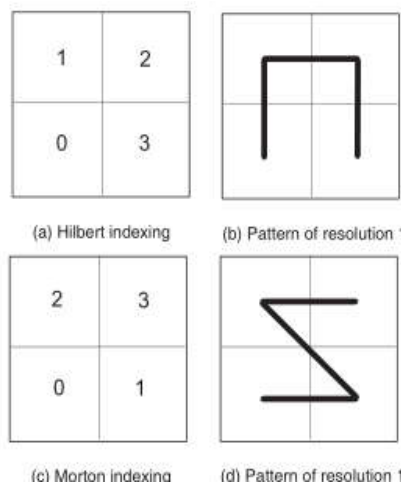


Figure 3. Indexing at resolution 1 for Hilbert and Morton curves

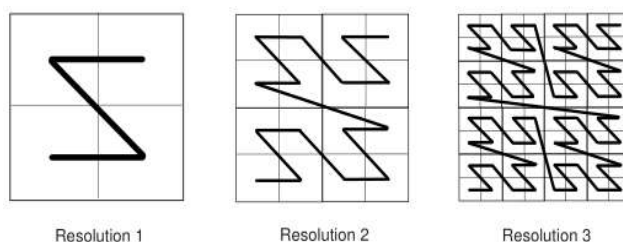


Figure 4. Morton's Space-Filling Curve

In order to discuss the number of Morton-type space-filling curves, first we note that from the Z (reversed) pattern of resolution 1 of the Morton curve, it can be obtained by geometrical transformations patterns only of: N, Z and N (reflected). In Figure 5 are shown the elemental transformations from the original Z (reversed) pattern of resolution 1 to the possible patterns for N, Z and N (reflected) also at resolution 1. The composition of functions of Table 1 with functions given on Figure 5 provides us the complete set of transformations to deduce all the possible configuration at resolution 2. Each one of these configurations is denoted by four letters in brackets belonging to $\{Z \text{ (reversed)}, Z, N, N \text{ (reflected)}\}$. For example let (ABCD) one of these configurations. Then (ABCD) means a resolution 2 pattern for the Morton space-filling given by A in quadrant 0, B in quadrant 1, C in quadrant 2, and D in quadrant 3. Pattern (ABCD) of resolution 3 will be denoted by $(ABCD)_3$ and will be understood as follows: $(ABCD)_3 = (A_2B_2C_2D_2)$ which means that pattern of resolution 3 is obtained by joining four patterns of resolution 2 in Z (reversed) order. The basic-blocks used in resolution 3 are shown in Figure 6. They are named in the figure as Z (reversed)-block, Z-block, N (reflected)-block, and N-block. Since they are resolution 2 these blocks can be also named as $Z \text{ (reversed)}_2, Z_2, N \text{ (reflected)}_2,$ and N_2 .

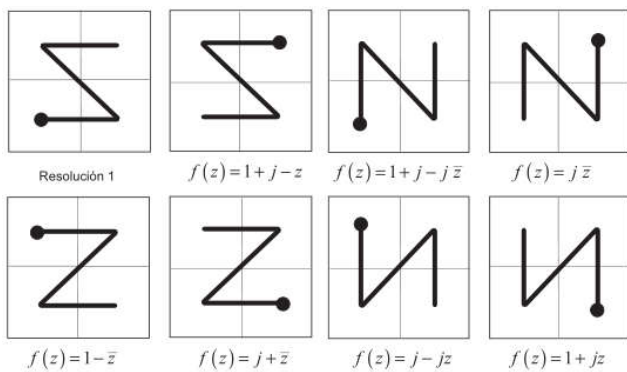


Figure 5. Elemental transformations used for Morton-type space-filling curves

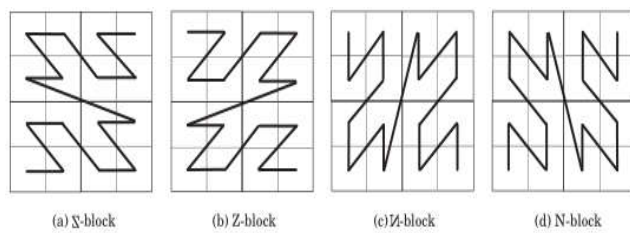


Figure 6. Basic blocks used at resolution three for Morton-type curves

Theorem 2.1. There are exactly 64 Morton-type space filling curves.

Proof: It is clear that the curve cross itself from quadrant 1 to quadrant 2, see Figure 7, if configurations Z (reversed) or N are in quadrants 1 or 2. This implies that Z and N (reflected)-block configurations are not valid for these quadrants, while Z (reversed) and N configurations are permitted. For the other two quadrants, 0 and 3, all possible configurations are valid. So, the total number of possible Morton-type space filling curves is $4 \cdot 2^2 \cdot 4 = 64$

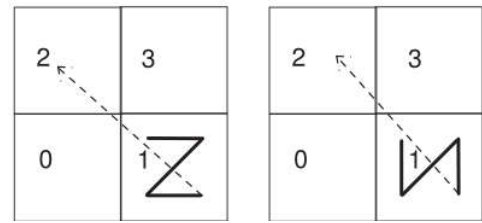


Figure 7. Invalid Morton-type configurations when the curve overlap at quadrant 1

Six of the 64 Morton-type space filling curves at resolution 2 and 3 are shown in Figure 8. However, since the rotation of π radians of Z (reversed), Z, N (reflected), and N is the only transformation that respectively yields Z (reversed), Z, N (reflected), and N, two patterns will be considered equivalent if the rotation of one of them gives the other.

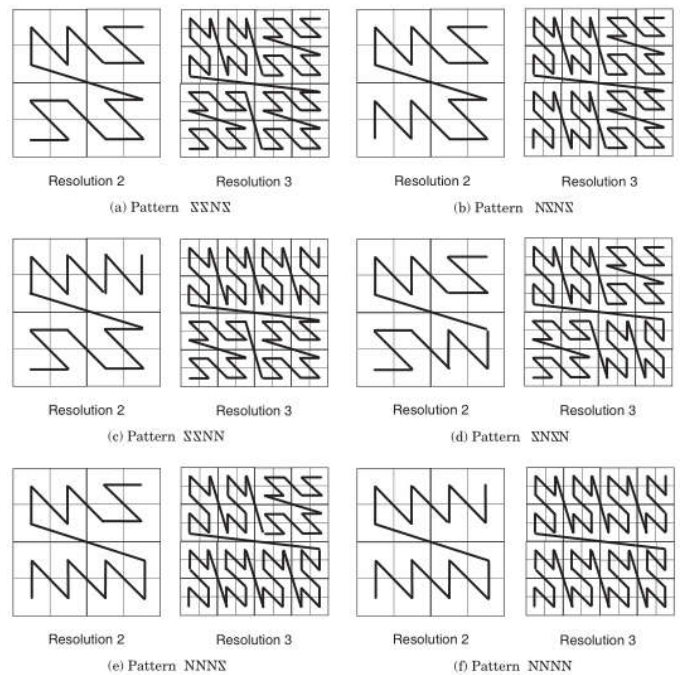


Figure 8. Some new patterns for Morton-type space-filling curves

Definition 2.2. Two Morton-type patterns $P_1 = (ABCD)$ and $P_2 = (A^*B^*C^*D^*)$ are equivalent if there is the rotation of π radians of one of them gives the other. That is, $P_1 \equiv P_2$ if and only if $P_1^{-1} = (ABCD)^{-1} = (DCBA) = (A^*B^*C^*D^*)$. A Morton-type pattern $P_1 = (ABCD)$ will be called a mirror pattern if $P_1^{-1} = P_1$, that is if $A = D$, and $B = C$. Note that a mirror pattern is ‘symmetrical’ like (ABBA), that remains the same when its letters are reversed. For example, pattern (Z (reversed) N Z (reversed)N) is equivalent to pattern (N Z (reversed) N Z (reversed)) (see Figure 8 (b) and (d)). Note, that by the identification of equivalent patterns it is easy to calculate the number of non equivalent Morton-type patterns as follows:

Proposition 2.3. There are 36 non equivalent Morton-type patterns.

Proof. The number of valid Morton-type patterns is 64. There are $4 \cdot 2 = 8$ mirror patterns. For each non mirror pattern P, P^{-1} is also another pattern equivalent to P . Therefore the number of non equivalent Morton-type patterns is $8+64 - 82= 36$.

It is feasible to design new curves with given constraints other than Hilbert, Moore or Morton patterns. Even among these families of curves, it has been paid attention to alternative patterns that introduce new type of curves. It is also possible consider other regular lattices (triangular, hexagonal) as they support space filling systems. It is difficult to devise an algorithm to automatically generate sets of space-filling curves. However, following the experience in this paper, we next provide general steps to construct more space-filling curves.

- Determine the alphabet (pattern of resolution 1) to construct the curve.
- Use Line segments and appropriate directions to fill a 2x2 cell.
- Determine patterns of resolution 2: the basic-block.
- List all traversals at resolution 2.
- Find all valid configuration of basic-blocks. (Theorem 1).
- Discard equivalent configurations (by rotations and mirrors).

Analysis of mechanical properties of bone models obtained by tac

The mechanical properties prediction on human bone models obtained by CT (Computerized Tomography) is one important aim to characterize the bone structural features and its tensional-deformational behavior.

The bone models are obtained from multiples CT cross-sectional images with a fixed distance, which are stored in graphic format DICOM (Digital Imaging and Communications in Medicine). To obtain the human bone model a segmentation process (collection of pixels in gray values equivalent to Hounsfield units) named thresholding were computed and bone contour curves was plotted. The threshold value makes it possible to select the bone tissue of the scanned patient (visualized by a green colored mask Figure 9).

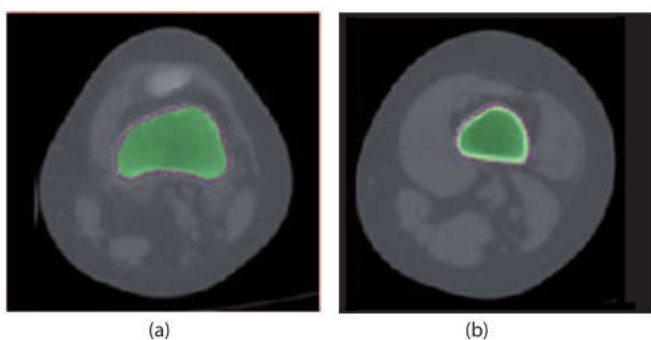


Figure 9. Thigh right leg CT images. Femur bone contour curves and bone tissue segmentation mask

The all created bone contour curves along the bone length display a 3D representation. Figure 10 shows the femur bone 3D modeling from CT cross-sectional images. To perform the material assignment to the bone 3D model we will convert this grayvalue/Hounsfield units to material properties. Many authors (Hobatho, Rho, and Ashman, 1997; Rho, Hobatho, and Ashman, 1995) reported from experimental values that the mechanical properties (Elastic Modulus and Poisson Ratio) of bone models can be estimated using the bone density values.

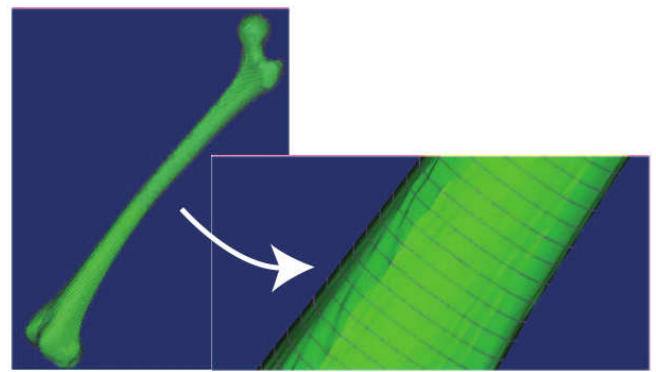


Figure 10. Femur bone 3D modeling from CT cross-sectional images

The mechanical property estimation can be calculated from CT cross-sectional images p pixel by using the following equations:

$$\text{Bone Density}(p) = -13.4 + 1017 * \text{GreyScale}(p) \tag{1}$$

$$\text{ElasticityMod}(p) = -388.8 + 5925 * \text{Density} \tag{2}$$

$$\text{PoissonRatio}(p) = -188.8 + 3425 * \text{Density} \tag{3}$$

Where Grayscale or Hounsfield unit equivalent is the p pixel value in the CT cross- sectional image.

The aim of this study are focused on Morton space-filling curve modeling, we propose a new method to accelerate the mechanical property estimation on bone contour curves from CT cross-sectional images. An adaptive SFC is needed to approximate a geometric domain and a tree data structure represented as a set of linked nodes (starting at a root node) throughout the CT cross-sectional bone area. For this goal we designed the algorithm SFC – bone, which takes as an entry the succession l_i of grey scale images with the bone cuts and the ϵ_i values that define the desire precision for the Morton curve. The algorithm output will be a geometric bone model, the Space-Filling curve SFC_i . The obtained model represent the traversal of the input cut images l_i , as well as the tree data structure represented as a set of linked nodes with the calculated bone mechanical properties: Density, Elastic Modulus and Poisson Ratio.

The SFC – bone algorithm is organized as follows: the first step computes the contours C_{ij} of each grey scale input image l_i . Many single contours can arise for a given image, as is the case for example of the head of a femur, where two or three separates contours may appear naturally from the bone geometry. In that case we have the information (nodal tree data structure) for each contours, which are represented in the algorithm with the index j as C_{i1} , C_{i2} , C_{i3} . It can be noted that computing contours is a well studied problem in the Computer Graphics. In the step 2 it is defined the Morton’s curve pattern which will be used as the basis of the curve generation. Those patterns can be of the form Z (reversed)-block, Z-block, N (reflected)-block, and N-block. In the third and four steps we are determining the Quadtree data structure Q_{ij} , where i represents the image that represents the bone cut and j the separated contour within each bone cut. See in Figure 11 an example of Quadtree for a femur cut. In relation to the precision it must be noted that this one will be as much, the resolution of the image in pixels. The loop in the fifth step

iteratively generates the Space Filling Curve SFC_{ij} . Step 7 computes the bone properties according to equations 1, 2 and 3. After processing each iteration on C_{ij} in the loop of step four, the last segment of the curve in C_{i-1} is joined to the corresponding starting point of curve in the C_i , creating so a linked list with a continuous curve for each bone cut, step seven in the algorithm, see Figure 12 and Figure 13.

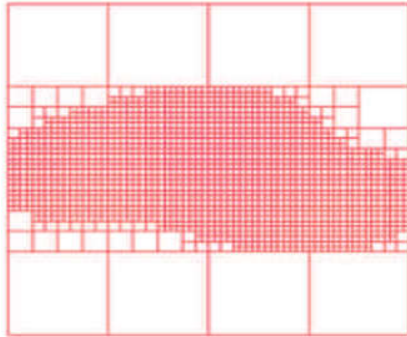


Figure 11. Femur bone Quadtree layer

Algorithm SFC-bone (I_i, ϵ_i, SFC_i)

/* **Input:** I_i images in grey tone representing bones; ϵ_i Choose precision for the Morton Curve

/* **Output:** Bone geometric model: SFC_i containing the Morton curve with information of Density, Elasticity modulus and Poisson ratio.

- 1: Let C_{ij} be the bone contours of I_i
- /* If $j > 1$ then there are several contours for I_i
- 2: Let N-Block be the chosen pattern for generating the Morton curve
- 3: For each C_{ij} do
- /* Compute the quadtree from the contours C_{ij} ...
- 4: Let Q_{ij} be the Quadtree of C_{ij} with precision ϵ_i
- 5: While $Q_{ij} \neq \emptyset$ do
- 6: Generate the Morton curve SFC_{ij}
- 7: Compute Density, Elasticity modulus and Poisson ratio.
- End while
- 8: Join the of starting SFC_{ij} with the previous curve

Endfor

End

The algorithm implementation run on AutoCAD graphical editor using AutoLISP application programming interface. AutoLISP is a programming language designed to extend and personalize the AutoCAD functionality. It based in the LISP programming language, which has its origins in the latest 50s. One of the AutoLISP advantages is the manipulation of graphical entities as association lists in AutoCAD. In AutoLISP the data type List is a group of values doubly linked, separated by spaces and closed by tween brackets.

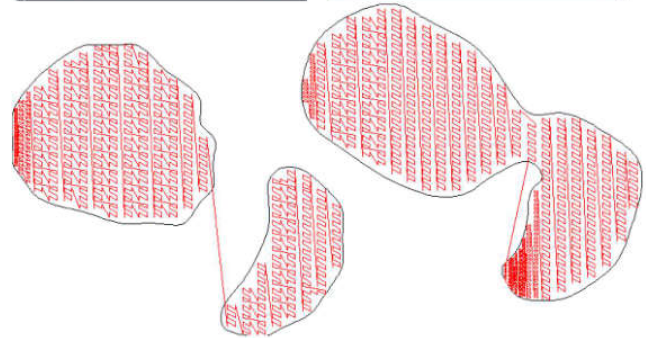
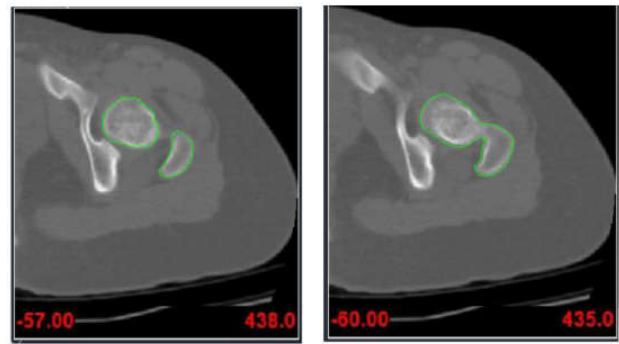


Figure 12. SFC generated from separated bone cut contours

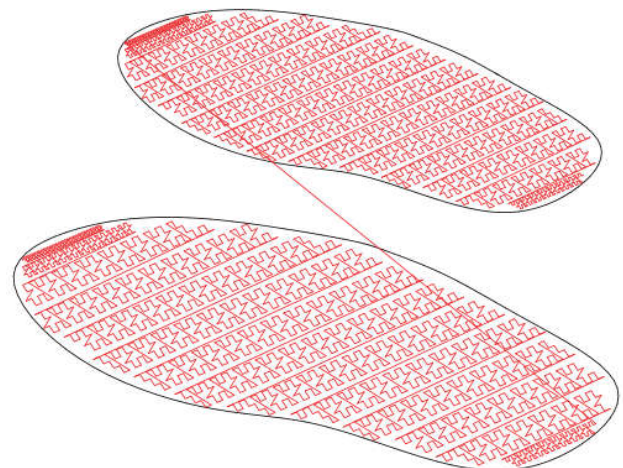


Figure 13. SFC generated from separated 3D bone cut contours

Lists are efficient data structures able to keep information of numerous related values, as is the case of the Morton curve in the bone cuts. It should be noted that one main advantage of testing the algorithm in AutoCAD is that it has permitted the use of the CAD environment, especially to the bone images import-processing and the powerful multilayer graphic environment for edition-visualization purposes.

Conclusions

Morton-type space-filling curves have been explored in several fields of engineering and computing, including PDEs solution by the Finite Element Method, algebraicmultigrid, data indexing and ordering. Our study determine new geometric patterns of utility to these fields. In this paper, we propose an algorithm to obtain a geometric model based in the Morton Curve from a sequence of bone cuts images. Also, we have presented the 64 different Morton filling-space curves patterns. This patterns has been written also to a simple transformation of the original reflect boxZ pattern to the classic Morton curve in resolution 1 in the Z (reversed), Z, N (reflected), and N that are the unique local patterns that emerge from geometric

transformations. Besides it has been identified the 36 no equivalents patterns. The algorithm suggested, and the Morton curve variations presented have been applied to obtain bone models and perform the mechanical properties analysis. It has to be highlighted that mechanical properties analyze means to find specific numerical parameters, as density, elastic modulus and Poisson ratio, in an efficient way inside the bone contour. To solve this, a model based in the meshes is not suitable, due to the searches and tours complexity in a volumetric mesh. An efficient and simple tool which allows to calculate the bone properties is offered with the model proposed.

REFERENCES

- Burgarelli, D., Kischinhevsky, M. and Biezuner, R. J. 2006. A new adaptive mesh refinement strategy for numerically solving evolutionary PDE's. *Journal of Computational and Applied Mathematics*, 196(1), 115-131. doi: <http://dx.doi.org/10.1016/j.cam.2005.08.013>
- Chen, H.-L., and Chang, Y.-I. 2005. Neighbor-finding based on space-filling curves. *Inf. Syst.*, 30(3), 205-226. doi: 10.1016/j.is.2003.12.002
- Erickson, P. K. A. y. J. 1999. Geometric range searching and its relatives, in *Advances in Discrete and Computational Geometry* (Bernard Chazelle, Jacob E. Goodman, and Richard Pollack, Eds.). *Contemporary Mathematics*, 223, 56.
- Evans, W., Kirkpatrick, D., and Townsend, G. 2001. Right-Triangulated Irregular Networks. *Algorithmica*, 30(2), 264-286. doi: 10.1007/s00453-001-0006-x
- Hilbert, D. 1891. Ueber die stetige Abbildung einer Linie auf ein Flächentstück. *Math Annln*, 38.
- Hobatho, M. C., Rho, J. Y., and Ashman, R. B. 1997. Anatomical variation of human cancellous bone mechanical properties in vitro. *Studies in health technology and informatics*, 40, 157-173.
- Liu, X. 2004. Four alternative patterns of the Hilbert curve. *Appl. Math. Comput.*, 147(3), 741-752. doi: 10.1016/s0096-3003(02)00808-1
- Moore, E. H. 1900. On Certain Crinkly Curves. *Transactions of the American Mathematical Society*, 1(1), 72-90. doi: 10.2307/1986405
- Morton, G. M. 1966. A computer oriented geodetic data base and a new technique in file sequencing. Ottawa: International Business Machines Co.
- Pajarola, R. W., Peter. 2001. Virtual Geoexploration: Concepts and Design Choices. *International Journal of Computational Geometry and Applications*, 11(01), 1-14. doi: 10.1142/s0218195901000389
- Pajarola, R., Antonijuan, M., and Lario, R. 2002, 1-1 Nov. 2002. QuadTIN: quadtree based triangulated irregular networks. Paper presented at the IEEE Visualization, 2002. VIS 2002.
- Peano, G. 1890. Sur unecourbe, qui remplitouteuneaire plane. *Mathematische Annalen*, 36(1), 157-160. doi: 10.1007/bf01199438
- Plaza, A., Suárez, J. P., and Padrón, M. A. 2005. Fractality of refined triangular grids and space-filling curves. *Engineering with Computers*, 20(4), 323-332. doi: 10.1007/s00366-004-0301-7
- R. Pajarola, P. W. 2000. An image compression method for spatial search. *IEEE Trans. Image Process*, 9.
- Rho, J. Y., Hobatho, M. C., and Ashman, R. B. 1995. Relations of mechanical properties to density and CT numbers in human bone. *Medical Engineering and Physics*, 17(5), 347-355. doi: [http://dx.doi.org/10.1016/1350-4533\(95\)97314-F](http://dx.doi.org/10.1016/1350-4533(95)97314-F)
- Sagan, H. 1994. *Space-Filling Curves* (Springer-Verlag Ed.). Berlin: Springer-Verlag.
- Song, Z., and Roussopoulos, N. 2000. Using Hilbert curve in image storing and retrieving. Paper presented at the Proceedings of the 2000 ACM workshops on Multimedia, Los Angeles, California, USA.
